Neutrino Fluxes from a Core-Collapse Supernova in a Model with Three Sterile Neutrinos

A. V. Yudin,[1,*] D. K. Nadyozhin,[1,†] V. V. Khruschov,[2,3,‡] and S. V. Fomichev[2,4,§]

[1] *Institute for Theoretical and Experimental Physics, Bolshaya Cheremushkinskaya 25, Moscow, 117218 Russia*
[2] *National Research Center Kurchatov Institute, Academician Kurchatov Place 1, Moscow, 123182 Russia*
[3] *Center for Gravitation and Fundamental Metrology, VNIIMS, Ozernaya Street 46, Moscow, 119361 Russia*
[4] *Moscow Institute of Physics and Technology (State University), Institutskii Lane 9, Dolgoprudnyi, Moscow Region, 141700 Russia*

arXiv:1701.04713v1 [astro-ph.HE] 16 Jan 2017

The characteristics of the gravitational collapse of a supernova and the fluxes of active and sterile neutrinos produced during the formation of its protoneutron core have been calculated numerically. The relative yields of active and sterile neutrinos in core matter with different degrees of neutronization have been calculated for various input parameters and various initial conditions. A significant increase in the fraction of sterile neutrinos produced in superdense core matter at the resonant degree of neutronization has been confirmed. The contributions of sterile neutrinos to the collapse dynamics and the total flux of neutrinos produced during collapse have been shown to be relatively small. The total luminosity of sterile neutrinos is considerably lower than the luminosity of electron neutrinos, but their spectrum is considerably harder at high energies.

Keywords: active and sterile neutrinos, neutrino oscillations, neutrino–matter interaction, supernova, collapse

INTRODUCTION

During the gravitational collapse of supernova cores the bulk of the released energy is carried away by powerful neutrino fluxes. Neutrinos of various flavors are produced both through a large number of processes involving nucleons and nuclei of stellar matter and due to neutrino oscillations, i.e., the conversion of one neutrino flavor into another. A peculiar feature of the oscillations of known neutrino flavors (electron, muon, and tau) in matter is their dependence on the electron number density distribution and the emergence of Mikheev–Smirnov–Wolfenstein (MSW) resonances. In those regions of stellar matter where the conditions for the emergence of MSW resonances are satisfied, the transition of one neutrino flavor to another is enhanced even if the initial vacuum mixing between different neutrino flavors was insignificant. Apart from the oscillations of known active neutrinos (AcN: electron, muon tau), the oscillations involving sterile neutrinos (StN) that do not interact directly with Standard Model (SM) particles through photon, W and Z boson, and gluon exchanges can occur.

The StN existence problem is a topical problem of modern neutrino physics. In particular, it relates to the anomalies of the neutrino and antineutrino fluxes at small distances in a number of ground-based experiments (see Abazajian et al. 2012; Schwetz et al. 2011; Giunti et al. 2013; Kopp et al. 2013; Gorbunov 2014). The presence of such anomalies, if it will be confirmed at a sufficient confidence level, is beyond the scope of the SM and the minimally extended SM (MESM) with three active massive neutrinos, because a new type of neutrinos, namely sterile neutrinos with a mass scale of ~ 1 eV, is required to explain them. In principle, the StN masses can lie within a wide range, from 10^{-5} eV to 10^{15} GeV (de Gouvea 2005; Drewes and Garbrecht 2015). It is convenient to divide this range in such a way that StN with masses less than 0.1 eV, from 0.1 to 100 eV, from 100 eV to 10 GeV, and more than 10 GeV to be assigned to the classes of superlight, light, heavy, and superheavy StN, respectively.

Phenomenological models with one, two, and three StN have been proposed to take into account StN (see Abazajian et al. 2012; Schwetz et al. 2011; Giunti et al. 2013; Kopp et al. 2013; Gorbunov 2014; Canetti et al. 2013; Conrad et al. 2013). If we take into account the possible left–right symmetry of weak interactions and associate the sterile neutrinos with the right neutrinos neutral with respect to $SU(2)_L$ weak interactions, then there must be three StN, i.e., $(3+3)$ models with three AcN and three StN should be considered (Canetti et al. 2013; Conrad et al. 2013). One of such models is the $(3+1+2)$ model (or $(3+2+1)$ model) that contains three StN, two of which are approximately degenerate in mass, while the mass of the third one can differ significantly from the masses of the two other ones (Zysina et al. 2014; Khruschov and Fomichev 2015). Within the $(3+2+1)$ model with three StN the AcN and

* yudin@itep.ru
† nadezhin@itep.ru
‡ khruschov_vv@nrcki.ru
§ fomichev_sv@nrcki.ru

StN mass characteristics were estimated (Zysina et al. 2014), the AcN and StN appearance and survival probabilities in the Sun were calculated by taking into account the coherent scattering of neutrinos in matter (Khruschov and Fomichev 2015), and various AcN and StN mixing matrices were considered to explain the neutrino anomalies at small distances (Khruschov et al. 2016).

Khruschov et al. (2015) considered the change in neutrino flavor composition due to coherent neutrino scattering by electrons and neutrons of superdense matter in the model with three StN. Allowance for neutrons does not lead to a change in oscillation characteristics if only AcN are considered. If the contribution of StN is taken into account, then the influence of the neutron density of matter becomes noticeable. In this paper it was shown that when the neutron-to-proton ratio is close to two, the StN yield is enhanced considerably. Such an enhancement arises at high or ultrahigh densities of matter; therefore, this effect can be of importance only in astrophysical conditions, for example, during the formation of a protoneutron supernova core. In models involving StN this effect is additional to the MSW effect and can lead to new consequences during supernova explosions. Despite the fact that the influence of StN on the processes in supernovae have been considered in many papers (see, e.g., Hidaka and Fuller 2006, 2007; Tamborra et al. 2012; Warren et al. 2014), the effect of an enhancement of the StN yield at a neutron-to-proton ratio in matter $\theta_{\rm n} \equiv n_{\rm n}/n_{\rm p} \approx 2$ was not studied in detail, although it was pointed out, for example, in Wu et al. (2014).

In models with three AcN and three StN there are difficulties in reconciling the number of neutrinos with cosmological observations. The observations of cosmological cosmic microwave background fluctuations within the framework of standard cosmological models limit the number of new light neutrinos virtually to one (see, e.g., Komatsu et al. 2011; Ade et al. 2013). Nevertheless, just as in Zysina et al. (2014), Khruschov and Fomichev (2015), and Khruschov et al. (2015, 2016), we will consider a model with three AcN and three StN. Let us list several reasons for such a choice. These include, first, the principle of left–right symmetry noted above, which may be restored on a scale exceeding the scale of spontaneous electroweak symmetry breaking, ~ 1 TeV. In addition, the form of the AcN and StN mixing matrix chosen under strict unitarity conditions in Khruschov et al. (2016) necessitates introducing three StN. Even if the derived cosmological constraints on the total number of relativistic neutrinos are taken into account, it should be noted that these constraints are model–dependent. Therefore, there must not be ruled out the possibility of the realization of nonstandard cosmological models within which, despite the existence of three StN, their effect will be reduced or virtually suppressed in the observational cosmological data, if other interaction and thermal equilibrium conditions for StN are assumed (see, e.g., Ho and Scherrer 2013; Chu et al. 2015).

The goal of this paper is to investigate the generation of sterile neutrinos during a supernova explosion. The paper is organized as follows. Initially, we provide information about the oscillation model used. Subsequently, we describe the procedures for calculating the production and propagation of sterile neutrinos that differ for the case of high opacity and the semitransparent case. We separately discuss the neutrino–neutrino scattering effect, which turns out to be important under conditions of an opaque and hot protoneutron star forming during a supernova explosion. We then present the results of our calculations for two chosen instants of time: at the phase of collapse and 3 ms after its stop and core bounce. We calculate the fluxes of sterile neutrinos and their spectra at the exit from the star. The physical conditions in the collapsing stellar core obtained in the hydrodynamic calculations by Yudin (2009), Yudin and Nadyozhin (2008), and Liebendörfer (2005) are taken into account in this case. In conclusion, we discuss our results and consider the possibilities of further studies in this area.

THE $(3+2+1)$ MODEL OF ACTIVE AND STERILE NEUTRINOS

Let us give the basic principles of the phenomenological $(3+2+1)$ model of neutrinos that is used below to calculate the effects involving three StN (Zysina et al. 2014; Khruschov and Fomichev 2015; Khruschov et al. 2015, 2016). In this model two StN are approximately degenerate in mass, while the mass of the third StN can differ significantly from the masses of the two other ones. Different StN flavors are denoted by indices x, y and z, while the additional massive states are denoted by indices $1'$, $2'$ and $3'$. The set of indices x, y and z is denoted by symbol s, while the set of indices $1'$, $2'$ and $3'$ is denoted by symbol i'. The general 6×6 mixing matrix $\widetilde{U}$ of AcN and StN can then be represented via 3×3 matrices S, T, V and W as

$$\left(\begin{array}{c}\nu_{\rm a}\\ \nu_{\rm s}\end{array}\right) = \widetilde{U}\left(\begin{array}{c}\nu_i\\ \nu_{i'}\end{array}\right) \equiv \left(\begin{array}{cc}S & T\\ V & W\end{array}\right)\left(\begin{array}{c}\nu_i\\ \nu_{i'}\end{array}\right). \quad (1)$$

The neutrino masses are specified in the form $\{m\} = \{m_i, m_{i'}\}$, with $\{m_i\}$ being arranged in direct order, i.e., $\{m_1, m_2, m_3\}$ and $\{m_{i'}\}$ being arranged in reverse order, i.e., $\{m_{3'}, m_{2'}, m_{1'}\}$. The unitary 6×6 matrix $\widetilde{U}$ is considered in a certain form under additional physical assumptions (Khruschov et al. 2016). As the basis of massive sterile states we choose the states for which the matrix W is approximately a unit one while restricting ourselves to a diagonal matrix of the form $W = \widetilde{\varkappa} I$, where I is a unit matrix and $\widetilde{\varkappa}$ is a complex parameter with a modulus close to unity,

$\widetilde{\varkappa} = \varkappa \exp(i\phi)$. We will represent the matrix S as $S = U_{PMNS} + \Delta U_{PMNS}$, with the matrices ΔU_{PMNS} and T being small compared to U_{PMNS}. For the convenience of our estimations of the mixing between AcN and StN and the corrections to the mixing only between AcN due to the influence of StN, we will assume that $\Delta U_{PMNS} = -\epsilon U_{PMNS}$, where ϵ is a small quantity, with $\epsilon = 1 - \varkappa$. The matrix S is then $S = \varkappa U_{PMNS}$, where U_{PMNS} is the well–known unitary 3×3 Pontekorvo–Maki–Nakagawa–Sakata mixing matrix ($U_{PMNS} U^{+}_{PMNS} = I$).

Thus, in the model under consideration at an appropriate normalization AcN are mixed via the matrix U_{PMNS}. At present, the most accurate values of the neutrino mixing parameters have been obtained in several papers (see, e.g., Olive et al. 2014; Capozzi et al. 2014). Since only the absolute value of the oscillation mass characteristic $\Delta m^2_{31} = m^2_3 - m^2_1$ is known, the absolute values of the neutrino masses can be ordered in two ways: *a*) $m_1 < m_2 < m_3$ and *b*) $m_3 < m_1 < m_2$, i.e., either normal hierarchy (NH, case a) or inverted hierarchy (IH, case b) of the neutrino mass spectrum is said to be realized. Given that the mixing between AcN and StN is small and is determined by the small parameter ϵ, we will choose the matrix T in the form$T = \sqrt{1 - \varkappa^2}\, a$ where a is an arbitrary unitary 3×3 matrix, $aa^{+} = I$. The unitary matrix $\widetilde{U}$ can then bewritten as

$$\widetilde{U} = \begin{pmatrix} \varkappa U_{PMNS} & \sqrt{1-\varkappa^2}\, a \\ -e^{i\phi}\sqrt{1-\varkappa^2}\, a^{+} U_{PMNS} & \varkappa e^{i\phi} I \end{pmatrix}. \tag{2}$$

Zysina et al. (2014), Khruschov and Fomichev (2015), and Khruschov et al. (2015) used an approximately unitary mixing matrix of form (2) at $\phi = 0$, where the condition for the conservation of the normalization of StN states was disregarded (for the corrections related to the nonunitarity of the mixing matrix, see, e.g., Antusch and Fischer 2014).

In this paper we will choose a trial value of the unknown phase ϕ as $\phi = \pi/4$. The matrix U_{PMNS} also contains an additional CP-phase δ_{CP}. Despite the fact that the CP-phase has not yet been established experimentally, it was estimated in several papers (see, e.g., Capozzi et al. 2014; Khruschov 2013; Petkov et al. 2015) for the normal hierarchy (NH) of the neutrino mass spectrum or, more specifically, $\sin\delta_{CP} < 0$ and $\delta_{CP} \approx -\pi/2$. The NH case is also more preferable when taking into account the constraints on the sum of the neutrino masses from cosmological observational data (Huang et al. 2015). Therefore, in our subsequent numerical calculations we will assume the NH case to be the main one and will use $\delta_{CP} = -\pi/2$ for it.

Khruschov et al. (2016) considered three forms of the matrix a for the NH case: a_1, a_2, and a_3. It was shown that in the forms a_1 and a_3 of the mixing matrix the transition probability of muon neutrinos/antineutrinos to electron neutrinos/ antineutrinos contains no contributions from StN, and, in both cases, the transition probabilities are identical and determined only by the AcN mixing parameters. In this paper we will consider the matrix a_2 written out below as the main one. This form leads to the dependence of the transition probabilities of muon neutrinos/antineutrinos to electron neutrinos/antineutrinos on the StN contributions and makes it possible to describe the experimentally revealed neutrino anomalies at small distances in principle. The matrix a_2 is

$$a_2 = \begin{pmatrix} \cos\eta_2 & \sin\eta_2 & 0 \\ -\sin\eta_2 & \cos\eta_2 & 0 \\ 0 & 0 & e^{-i\chi_2} \end{pmatrix}, \tag{3}$$

where χ_2 and η_2 are the phase and angle of mixing between AcN and StN. In our calculations we will use the following trial values of the new mixing parameters: $\chi_2 = -\pi/2$ and $\eta_2 = \pm 30^{\circ}$. We will constrain the small parameter ϵ by the condition $\epsilon \lesssim 0.03$.

We use the results from Zysina et al. (2014) and Khruschov and Fomichev (2015) referring to the estimates of the absolute values of the AcN masses m_i ($i = 1, 2, 3$) for the NH case in eV: $m_1 \approx 0.0016$, $m_2 \approx 0.0088$, $m_3 \approx 0.0497$. We choose the masses $m_{3'}$ and $m_{2'}$ of two StN near 1 eV in accordance with the results from Kopp et al. (2013) for the best StN masses in a $(3+2)$ model, i.e., $m_{3'} \approx 0.69$ eV and $m_{2'} \approx 0.93$ eV. For the mass $m_{1'}$ of the third StN we will use the mass of a possible dark matter (DM) particle taken from Bulbul et al. (2014), Boyarsky et al. (2014), and Horyuchi et al. (2015), i.e., $m_{1'} \approx 7100$ eV. Thus, the absolute values of the masses (in eV) of all neutrinos within this model are as follows:

$$m_\nu = \{0.0016,\, 0.0088,\, 0.0497,\, 0.69,\, 0.93,\, 7100\}. \tag{4}$$

Given this sterile neutrino mass distribution, the model with three sterile neutrinos under consideration may be called the (3+2+1) model of active and sterile neutrinos. Note that this model can in principle mimic the (3+1) and (3+2) models as one or two sterile neutrinos decrease in importance, for example, as their masses increase significantly or for a special choice of mixing angles.

To calculate the probability amplitudes for the propagation of neutrinos with certain flavors in a medium, we will use the equations from Khruschov and Fomichev (2014):

$$i\partial_r \begin{pmatrix} a_{\rm a} \\ a_{\rm s} \end{pmatrix} = \left[\frac{\tilde{\Delta}_{m^2}}{2E} + \sqrt{2} G_F \begin{pmatrix} \widetilde{N}_{\rm e}(r) & 0 \\ 0 & \widetilde{N}_{\rm n}(r)/2 \end{pmatrix} \right] \begin{pmatrix} a_{\rm a} \\ a_{\rm s} \end{pmatrix}. \tag{5}$$

Here, we introduce the matrix $\tilde{\Delta}_{m^2} = \tilde{U}\Delta_{m^2}\tilde{U}^T$, where $\Delta_{m^2} = \mathrm{diag}\{m_1^2 - m_0^2,\, m_2^2 - m_0^2,\, m_3^2 - m_0^2,\, m_{3'}^2 - m_0^2,\, m_{2'}^2 - m_0^2,\, m_{1'}^2 - m_0^2\}$, with m_0 being the smallest neutrino mass among m_i and $m_{i'}$. The matrices $\widetilde{N}_\mathrm{e}(r)$ and $\widetilde{N}_\mathrm{n}(r)$ are 3×3 matrices of the form

$$\widetilde{N}_\mathrm{e}(r) = \begin{pmatrix} n_\mathrm{e}(r) & 0 & 0 \\ 0 & 0 & 0 \\ 0 & 0 & 0 \end{pmatrix}, \tag{6}$$

$$\widetilde{N}_\mathrm{n}(r) = \begin{pmatrix} n_\mathrm{n}(r) & 0 & 0 \\ 0 & n_\mathrm{n}(r) & 0 \\ 0 & 0 & n_\mathrm{n}(r) \end{pmatrix}, \tag{7}$$

while n_e and n_n are the local electron and neutron number densities, respectively.

THE PROCEDURE FOR CALCULATING THE FLUX OF STERILE NEUTRINOS

Electron neutrinos from nonequilibrium neutronization of matter are mostly emitted during the collapse of an iron stellar core up to its stop and the generation of a diverging shock front. In this case, the fluxes of electron antineutrinos, along with neutrinos of other flavors (muon and tau ones), may be neglected at least for another several tens of milliseconds after core bounce. Below we will describe the procedure for calculating the generation of StN fluxes under these conditions. We will distinguish two cases: the case of high opacity with respect to electron neutrinos and the transparent one. A spherical symmetry is assumed with regard to the stellar core geometry. The following neutrino–matter interaction processes are taken into account in our calculations:

$\nu_\mathrm{e} + n \rightleftarrows p + e^-$**:** the neutrino absorption by a free neutron and the reverse process: the electron capture by a proton with neutrino emission;

$\nu_\mathrm{e} + (A, Z) \rightleftarrows (A, Z{+}1) + e^-$**:** the beta–processes on nuclei;

$\nu_\mathrm{e} + z \to \nu_\mathrm{e}' + z'$**:** $z = n$ or p — the elastic scattering by free nucleons;

$\nu_\mathrm{e} + (A, Z) \to \nu_\mathrm{e}' + (A, Z)'$**:** the coherent scattering by atomic nuclei. A very important source of opacity due to the quadratic dependence of the reaction cross section on the atomic weight of the target: $\sigma_\mathrm{cs} \propto A^2$;

$\nu_\mathrm{e} + e^- \to \nu_\mathrm{e}' + e'^-$**:** the inelastic neutrino scattering by electrons. An important process of thermalization of the neutrino radiation field.

The cross sections for these reactions were calculated by Burrows and Thompson (2002) and Yudin and Nadyozhin (2008) (for the neutrino scattering by an electron).

THE CASE OF HIGH OPACITY

When the density at the center of the stellar core during its collapse reaches $\rho \sim 10^{13}$ g/cm^{-3}, the neutrinos turn out to be trapped. In this case, the neutrinos propagate in the regime of diffusion, and the neutrino mean free path l_ν in matter is small compared to the characteristic length scales of the changes in thermodynamic parameters (for more details, see Imshennik and Nadyozhin 1972). The radius of this region in the star is commonly called the neutrinosphere, by analogy with the photosphere in ordinary stars. Let us consider how StN are generated under these conditions.

We will proceed from the fact that we have a function $P_\mathrm{st}(\omega_\nu, x)$ giving the probability that an electron neutrino with energy ω_ν, having traversed a distance x, oscillated into sterile states (see Khruschov et al. 2015). In this case, P_st also depends on the local thermodynamic parameters of matter such as the density, the degree of neutronization, etc. which are assumed to remain constant over the entire distance x. However, the function P_st disregards the neutrino absorption and scattering in matter, which "knock out" the neutrinos from the beam. Consider this effect in detail. Let we have a flux of electron neutrinos propagating in a specified direction. The change in flux with distance is described by the elementary solution of the transfer equation $F_\nu(x) = F_\nu(0)e^{-\lambda_\nu x}$, where $\lambda_\nu \equiv 1/l_\nu$ is the absorptivity. In this case, we disregard the neutrino emission and scattering into a "beam" on the path length,

because these neutrinos will be incoherent with the original ones and will not be involved in the oscillations. For the same reason, the opacity $\lambda_\nu(\omega_\nu)$ used here,

$$\lambda_\nu(\omega_\nu) = \lambda_{\rm abs}(\omega_\nu) + \int R^{\rm out}(\omega_\nu, \omega'_\nu, \eta)(1-f_\nu(\omega'_\nu))d\omega'_\nu d\Omega', \tag{8}$$

differs from its ordinary value $\widetilde{\lambda}_\nu$ corrected for the induced absorption (see Imshennik and Nadyozhin 1972) by the factor $\widetilde{\lambda}_\nu = \lambda_\nu/(1-f_\nu^{\rm eq})$, where $f_\nu^{\rm eq}$ is the equilibrium neutrino distribution function at a given point. In Eq. (8) the first and second terms describe the neutrino absorption and scattering processes, respectively, $R^{\rm out}$ is the scattering kernel dependent on the energy of the initial neutrino ω_ν, the scattered neutrino ω'_ν, and the cosine of the angle between them η, while the integration is over the energy and direction of the scattered neutrino (for more details, see Yudin and Nadyozhin 2008). Note that the neutrino distribution function $f_\nu(\omega'_\nu)$ is not necessarily an equilibrium and isotropic one in the general case and, in general, must be found from the solution of the transport equation. However, under the conditions we consider, inside the opaque region, the neutrino distribution is very close to an equilibrium one.

Let us return to the consideration of the StN generation. The fraction $P_{\rm st}(x+dx)-P_{\rm st}(x)$ from the electron neutrinos that traversed a distance x oscillate into sterile states in the range $(x \div x+dx)$. The total StN flux generated by the flux of electron neutrinos propagating in the medium is then

$$F_{\rm st} = \int\limits_0^\infty F(x)\frac{dP_{\rm st}(x)}{dx}dx = F(0)\int\limits_0^\infty P_{\rm st}(x)\lambda_\nu e^{-\lambda_\nu x}dx. \tag{9}$$

As can be seen from (9), we can introduce a function $G_{\rm st}(\omega_\nu)$ that defines the fraction of neutrinos from the original beam that oscillated into sterile states:

$$G_{\rm st}(\omega_\nu) \equiv \int\limits_0^\infty P_{\rm st}(x,\omega_\nu)e^{-x/l_\nu(\omega_\nu)}\frac{dx}{l_\nu(\omega_\nu)} \le 1, \tag{10}$$

where we used the identity $\lambda_\nu \equiv 1/l_\nu$. The oscillation length is seen to be effectively limited by a quantity of the order of l_ν. Naturally, apart from the neutrino energy, the function $G_{\rm st}$ also depends on the remaining local parameters of matter. When deriving Eq. (10), we, first, assumed that $P_{\rm st}(x) \ll 1$, a condition that holds good in the case under consideration. Indeed, for a reasonable choice of oscillation model parameters the only region in the star where the oscillation probability can be comparable to unity is the resonance (in degree of neutronization $\theta_{\rm n}$) zone (see Khruschov et al. 2015). However, the electron neutrino must have traversed a distance much greater than the mean free path l_ν to oscillate into sterile states with a high probability even in this case. Second, we assumed that the parameters of matter did not change significantly at distances of the order of the mean free path. Thus, in particular, the condition for the density gradient in the star

$$\left|\frac{d\ln\rho}{dr}\right| \; l_\nu \ll 1, \tag{11}$$

and the analogous conditions for the remaining thermodynamic quantities must hold. As our calculations show, these conditions actually hold inside the neutrino opacity region in the collapsing stellar core.

Let us now turn to the calculation of the neutrino flux emitted from a unit volume of matter. This flux is determined by the emissivity entering into the transport equation (see Yudin and Nadyozhin 2008),

$$\kappa_\nu(\omega_\nu) = (1-f_\nu(\omega_\nu))\left[\lambda_\nu(\omega_\nu)e^{\frac{\mu_\nu-\omega_\nu}{kT}} + \int R^{\rm in}(\omega_\nu,\omega'_\nu,\eta)f'_\nu(\omega'_\nu)d\omega'_\nu d\Omega'\right]. \tag{12}$$

Here, the first and second terms in square brackets are responsible for the neutrino emission and scattering into a beam, respectively, μ_ν is the neutrino equilibrium chemical potential, and the factor $(1-f_\nu)$ describes the reduction of the phase space due to the Pauli exclusion principle. It is easy to verify that the Kirchhoff law holds: in equilibrium, when $f_\nu = f_\nu^{\rm eq}$,

$$\kappa_\nu = f_\nu^{\rm eq}\lambda_\nu. \tag{13}$$

In particular, this is ensured by the symmetry properties of the scattering kernel (Yudin and Nadyozhin 2008),

$$R^{\rm in}(\omega'_\nu,\omega_\nu,\eta) = R^{\rm out}(\omega_\nu,\omega'_\nu,\eta), \quad R^{\rm in}(\omega_\nu,\omega'_\nu,\eta) = e^{\frac{\omega'_\nu-\omega_\nu}{kT}}R^{\rm out}(\omega_\nu,\omega'_\nu,\eta). \tag{14}$$

Given the emissivity per unit volume of matter and the fraction of neutrinos oscillating into sterile states defined by the function $G_{\rm st}(\omega_\nu, r)$ (10), we can find the StN energy flux at radius r in the star (see Ivanova et al. 1969):

$$F_\nu^{\rm st}(r) = \int\limits_0^\infty \frac{\omega_\nu^3 d\omega_\nu}{h^3c^2} \int\limits_0^r \kappa_\nu(\omega_\nu, r') G_{\rm st}(\omega_\nu, r') \frac{4\pi r'^2}{r^2} dr'. \tag{15}$$

The local StN number density can also be calculated:

$$n_\nu^{\rm st}(r) = \int\limits_0^\infty \frac{\omega_\nu^2 d\omega_\nu}{h^3c^3} \int\limits_0^{R_{\rm s}} \kappa_\nu(\omega_\nu, r') G_{\rm st}(\omega_\nu, r') \frac{2\pi r'}{r} \ln\left|\frac{r+r'}{r-r'}\right| dr'. \tag{16}$$

Note that the integral in (16) is taken over the entire star, while the integral in (15) is taken only to the current radius r. These expressions allow all the StN flux characteristics of interest to us in the neutrino opacity region to be found.

THE REGION OUTSIDE THE NEUTRINOSPHERE

To calculate the StN generation in semitransparent and transparent regions, i.e., where the electron neutrino mean free path is comparable to or greater than the characteristic length scales of the changes in thermodynamic quantities, we first solve the transport equation for electron neutrinos. The peculiarities of the numerical scheme that we use can be found in Nadyozhin and Otroshchenko (1980). Thus, we determined the neutrino radiation field and, in particular, the emissivity κ_ν. However, in our case, apart from the radial coordinate r and energy ω_ν, the latter also depends on the direction, i.e., on the direction cosine η.

The same is also true for the function $G_{\rm st}$ defining the fraction of electron neutrinos oscillated into sterile states: $G_{\rm st} = G_{\rm st}(\omega_\nu, r, \eta)$. Let us describe the algorithm of finding it in this case. In each computational domain with coordinate r we determine the set of directions, i.e., the direction cosines η_i, $(i = 1 \div 6)$, chosen as the grid points of Legendre polynomials for the subsequent numerical integration using a 6-point scheme. The equation for the propagation of a beam of electron neutrinos with a given energy ω_ν through the star is numerically solved along each of the directions. Initially, the normalized set of fluxes of all neutrino flavors is $\vec{F}_\nu \equiv \{F_{\rm e}, F_\mu, F_\tau, F_{\rm x}, F_{\rm y}, F_{\rm z}\} = \{1, 0, 0, 0, 0, 0\}$. In each computational interval in the star the flux of electron neutrinos decreases due to their absorption and scattering: $F_{\rm e}' = F_{\rm e} e^{-\triangle l/l_\nu}$ where $\triangle l$ is the length of the interval along the propagation path (recall that we disregard the reverse processes, i.e., the emission and scattering into a beam, because these neutrinos will be incoherent with the original ones). Thereafter, we determine the redistribution of fluxes between the neutrino flavors using the function $P_{\rm st}(\omega_\nu, \triangle l)$. By considering $P_{\rm st}$ as an operator, we can symbolically write $\vec{F}_\nu' = \widehat{P}_{\rm st}(\omega_\nu, \triangle l)\vec{F}_\nu$. The two processes described above, namely the knocking-out of neutrinos from the beam and the oscillation redistribution of flavors, allow the local value of the function $G_{\rm st}$ to be found. The computation is continued until the fraction of electron neutrinos in the beam drops below a certain level (we took 5% of the sum of the fluxes of all neutrino flavors) or until the stellar surface is reached.

We now have all information to calculate the StN energy flux at a distance r from the stellar center. The previous expression (15) must be replaced by the following integral (see Fig. 1 for an explanation):

$$F_\nu^{\rm st}(r) = \int\limits_0^\infty \frac{\omega_\nu^3 d\omega_\nu}{h^3c^2} \int\limits_0^{R_{\rm s}} \int\limits_{-1}^{1} \Upsilon_\nu^{\rm st}(\omega_\nu, r', \eta) \frac{2\pi r'^2 \cos\varphi}{l^2} dr' d\mu, \tag{17}$$

where we, for brevity, denoted $\Upsilon_\nu^{\rm st} \equiv \kappa_\nu G_{\rm st}$. Here, $\mu = \cos\theta$, $l^2 = r^2 + r'^2 - 2rr'\mu$, $\cos\varphi = (r - r'\mu)/l$, and $\eta = \cos\psi = (r\mu - r')/l$. Remarkably, the integration over the angles in (17) can be performed explicitly. Indeed, it is easy to show that

$$d\eta = d\left(\frac{r\mu - r'}{l}\right) = \frac{r^2\cos\varphi}{l^2} d\mu. \tag{18}$$

As μ changes within the range $(-1, 1)$ η changes from -1 to $(r - r')/|r - r'|$. This means that at $r' > r$ the integral over the angle in (17) is zero. Finally, we can write

$$F_\nu^{\rm st}(r) = \int\limits_0^\infty \frac{\omega_\nu^3 d\omega_\nu}{h^3c^2} \int\limits_0^r \Upsilon_{\nu 0}^{\rm st}(\omega_\nu, r') \frac{4\pi r'^2}{r^2} dr', \tag{19}$$

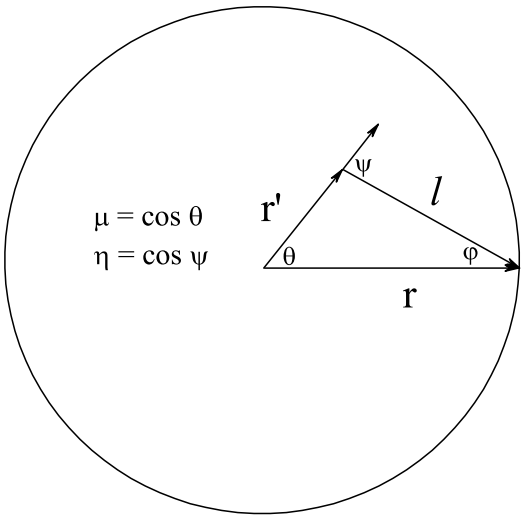

FIG. 1. Scheme to calculate the flux of sterile neutrinos.

where we introduced the following notation for the zeroth angular moment of $\Upsilon^{\rm st}_{\nu}$:

$$\Upsilon^{\rm st}_{\nu 0}(\omega_\nu, r') \equiv \frac{1}{2}\int\limits_{-1}^{1} \Upsilon^{\rm st}_{\nu 0}(\omega_\nu, r', \eta) d\eta. \tag{20}$$

It is important to note that, just as (15), our final expression for the flux (19) includes the integration only to the current r and not to the full stellar radius $R_{\rm s}$. In addition, a remarkable feature of Eq. (19) is that the quantity $\Upsilon^{\rm st}_{\nu}$, which, recall, is equal to the product of the emissivity of matter by the StN fraction, enters only by its minimal (zeroth) moment of the distribution. We perform the numerical angular integration in (20) using a six-point Gaussian scheme.

The $\nu_{\rm e}$–$\nu_{\rm e}$ SCATTERING EFFECT

So far we have taken into account only the neutrino scattering by the following components of matter when calculating the neutrino oscillation effects in the medium: neutrons, protons, and electrons. This led to the dependence of the interaction potential $V_{\rm s} \propto 3Y_{\rm e}-1$ (see, e.g., Abazajian et al. 2012), where $Y_{\rm e}$ is the ratio of the electron number density to the total number density of neutrons and protons. Given that $Y_{\rm e} = \frac{1}{1+\theta_{\rm n}}$, as would be expected, we obtain the critical value $V_{\rm s} = 0$ at $\theta_{\rm n} = 2$. However, if there is a considerable number of electron neutrinos in the medium (as in the opaque region of the central supernova core), then the possibility of neutrino–neutrino scattering should also be taken into account. This leads to a modification of the potential (see Blinnikov and Okun 1988): $V_{\rm s} \propto 3Y_{\rm e}-1+4Y_\nu$, where Y_ν is the dimensionless number density of electron neutrinos in the medium (see Eq. (23) below). Naturally, the oscillation function $G_{\rm st}$ begins to also depend on Y_ν in this case. The critical value of $\theta_{\rm n}$ is shifted to values greater than two:

$$\theta_{\rm cr} = 2 + \frac{12Y_\nu}{1-4Y_\nu}. \tag{21}$$

However, an important clarification should be made here: Eq. (21) and the above formula for the potential $V_{\rm s}$ containing Y_ν are valid only for an isotropic distribution of neutrinos. In our case, however, the angular neutrino distribution function can deviate greatly from an isotropic one. In particular, outside the neutrinosphere the neutrinos mostly propagate in a narrow solid angle in a direction away from the stellar center. Let us show how the expression for the critical degree of neutronization $\theta_{\rm cr}$ should be modified in this case.

To begin with, let us introduce the angular moments of the neutrino distribution function according to the definition

$$f_{\nu k} = \frac{1}{2}\int\limits_{-1}^{1} \mu^k f_\nu(\mu) d\mu, \tag{22}$$

where μ is the cosine of the angle between the neutrino propagation direction and the radius vector of a given point in the star. The quantity Y_ν is expressed via the zeroth moment of the distribution function as

$$Y_\nu = \frac{4\pi m_{\rm u}}{\rho (hc)^3}\int\limits_0^\infty \omega_\nu^2 f_{\nu 0}(\omega_\nu) d\omega_\nu, \tag{23}$$

where $m_{\rm u}$ is an atomic mass unit.

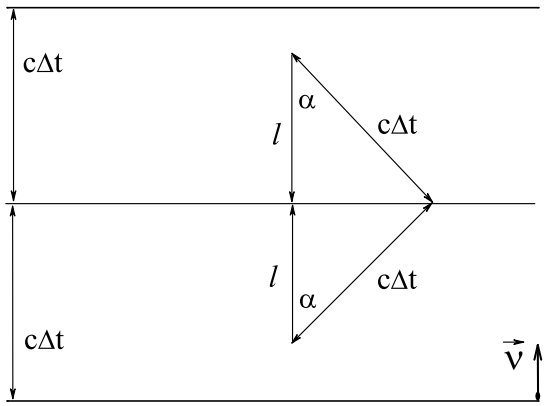

FIG. 2. Illustration to the calculation of $\theta_{\rm cr}$ when the $\nu_{\rm e}-\nu_{\rm e}$ scattering is taken into account.

Let us now consider a neutrino propagating with speed c for a time $\triangle t$ "upward" in Fig. 2. It can interact with all the neutrinos from the lower halfplane moving "downward". In addition, in the lower half–plane it can interact with the upward–moving neutrinos that were at a distance l from the middle line at $t = 0$ and whose propagation direction made an angle no smaller than α with the direction of the neutrino under consideration. Similarly, from the upper half–plane our neutrino can interact only with the neutrinos that propagate downward within the angle α (see Fig. 2). Thus, the quantity $4\pi f_{\nu 0}$ in (23) must be replaced by

$$\int\limits_{\Omega_1} f_\nu d\Omega + \frac{1}{c\triangle t}\int\limits_0^{c\triangle t}\left(\int\limits_{\Omega_2} f_\nu d\Omega + \int\limits_{\Omega_3} f_\nu d\Omega\right) dl, \tag{24}$$

where the integration over the solid angle Ω is within the following limits:

$$\begin{aligned} \Omega_1: &\quad (\vec{n}\vec{m}) \le 0, \\ \Omega_2: &\quad 0 \le (\vec{n}\vec{m}) \le \frac{l}{c\triangle t}, \\ \Omega_3: &\quad -1 \le (\vec{n}\vec{m}) \le -\frac{l}{c\triangle t}. \end{aligned} \tag{25}$$

Here $\vec{n}$ and $\vec{m}$ are unit vectors in the propagation directions of the original neutrino and the neutrino of the medium, respectively. Let us decompose the neutrino distribution function f_ν into its angular moments: $f_\nu = f_{\nu 0} + 3\mu f_{\nu 1} + O(\mu^2)$. The cosine of the angle μ can be expressed via the angle between the interacting neutrinos $\chi \equiv (\vec{n}\vec{m})$ and the direction cosine of the original neutrino η as

$$\mu = \chi\eta + \sqrt{1-\chi^2}\sqrt{1-\eta^2}\cos(\varphi_1 - \varphi_2). \tag{26}$$

This allows the integration in (24) to be performed analytically using the relation $d\Omega = d\varphi_2 d\chi$. The critical degree of neutronization now depends on the propagation direction of the neutrino under consideration, i.e., this is the function $\theta_{\rm cr}(\eta)$, and it is still defined by Eq. (21), but with Y_ν replaced by $\widehat{Y}_\nu(\eta)$, where

$$\widehat{Y}_\nu(\eta) = \frac{4\pi m_{\rm u}}{\rho(hc)^3}\int\limits_0^\infty \big(f_{\nu 0}(\omega_\nu) - \eta f_{\nu 1}(\omega_\nu)\big)\omega_\nu^2 d\omega_\nu. \tag{27}$$

Expression (27) is valid to within $O(f_{\nu 3})$, because the contribution of the second moment $f_{\nu 2}$ can be shown to be zero. In the opaque region $f_{\nu 1} \ll f_{\nu 0}$ and (27) is reduced to (23). In contrast, in the region high above the neutrinosphere $f_{\nu 1} \approx f_{\nu 0}$ and $\widehat{Y}_\nu(\eta)$ is highly anisotropic: if $\eta \approx 1$ then $\widehat{Y}_\nu(\eta) \approx 0$, because all neutrinos (including that under consideration) move nearly radially away from the stellar center without any interaction. On the other hand, at $\eta \approx -1$ the neutrino under consideration moves toward the flux of remaining neutrinos, and the interaction effect is doubled.

As we will show below, the $\nu_{\rm e}$–$\nu_{\rm e}$ scattering effect itself turns out to be very important in the calculations of the StN fluxes from supernovae. It can lead to both an increase and a decrease in the StN yield. Below we will distinguish three cases: the calculations without any scattering effect ($\theta_{\rm cr} = 2$), with isotropic scattering ($\theta_{\rm cr}$ is given by Eq. (21) with Y_ν determined from Eq. (23)), and with anisotropic scattering with Eq. (27) for $Y_\nu \equiv \widehat{Y}_\nu$ in Eq. (21) for $\theta_{\rm cr}$.

RESULTS

We used the results of hydrodynamic simulations for the collapse of an iron stellar core with a mass of $2M_\odot$ from Yudin (2009) as a basis for our calculations of the StN fluxes from a supernova. From the above paper we took the distributions of thermodynamic and hydrodynamic parameters of the core at various instants of time, starting from the instant the stellar core lost its stability up to several tens of milliseconds after bounce. This time interval corresponds to the formation of the first powerful peak of neutrino emission consisting mostly of electron neutrinos from nonequilibrium neutronization of matter. In this case, the degree of neutronization $\theta_{\rm n}$ increases from $\theta_{\rm n} \approx 1$ in the pre–collapse matter to $\theta_{\rm n} \approx 2.5$ in the central core region (see also Liebendörfer 2005), while in the neutronization region behind the expanding shock front (see Figs 3 and 6 below) $\theta_{\rm n}$ reaches even greater values. The collapsing matter, naturally, passes through the most interesting region of the critical degree of neutronization, i.e., the zone of a resonant enhancement of the neutrino oscillations.

THE PREBOUNCE COLLAPSE PHASE

Let us first consider the stellar core collapse phase before bounce and the formation of a diverging shock front. The distribution of parameters in the stellar core at the moment when the density of matter at the center is lower than the nuclear density $\rho_{\rm n} \approx 2.6 \times 10^{14}$ g/cm^{-3} by only several times is shown in Fig. 3. Figure 3a shows the temperature $T_9 \equiv T \times 10^{-9}$ K (solid curve, left axis) and the logarithm of the density $\lg \rho$ (dashed curve, right axis) as functions of the mass coordinate $m = M/M_\odot$. At $m \approx 0.85$ we can clearly see the formation of a density jump, the place where the future shock front is formed. Approximately the same mass coordinate separates the central neutronized part of the star with $\theta_{\rm n} > 2$ from the outer region with $\theta_{\rm n} \approx 1$ ($\theta_{\rm n}$ is indicated by the solid curve in Fig. 3b). The critical degrees of neutronization with allowance made for the $\nu_{\rm e}$–$\nu_{\rm e}$ scattering are also presented here. $\theta_{\rm cr}$ corresponds to the critical value for isotropic scattering, while $\theta_{\rm cr}^{\pm}$ corresponds to anisotropic scattering for $\eta = \pm 1$ in Eq. (27). In the outer part of the core $\theta_{\rm cr}$ and $\theta_{\rm cr}^-$ increase rapidly, because Y_ν increases. Indeed, $Y_\nu \equiv \dfrac{m_{\rm u} n_\nu}{\rho}$, where n_ν is the neutrino number density that drops with distance in the outer part approximately as $n_\nu \sim 1/r^2$. Since the density decreases more rapidly, Y_ν increases. This effect is compensated only for $\theta_{\rm cr}^+$, because in the outer region $f_{\nu 0} \approx f_{\nu 1}$ (see Eq. (27)).

Let us now consider the results of our calculations of the StN generation with this stellar profile. Figure 4 shows the spectral luminosities L_ν (erg s^{-1} MeV^{-1}) of neutrinos leaving the collapsing core. The curve with filled squares indicates the spectrum of electron neutrinos; the remaining curves indicate the spectra of the x, y, and z StN components. Figures 4a–4c correspond to the calculations without $\nu_{\rm e}$–$\nu_{\rm e}$ scattering, with isotropic scattering, and with anisotropic scattering, respectively. The spectra of the x and y components virtually coincide in the entire range of energies, except for the lowest ones ($E_\nu \lesssim 5$ MeV), while the yield of the z component is much smaller. The StN spectrum itself has a characteristic shape: it consists of a central part with a maximum at ~ 10 MeV and a broad "pedestal" with a considerably flatter spectrum at high energies. This part of the spectrum is attributable to the StN

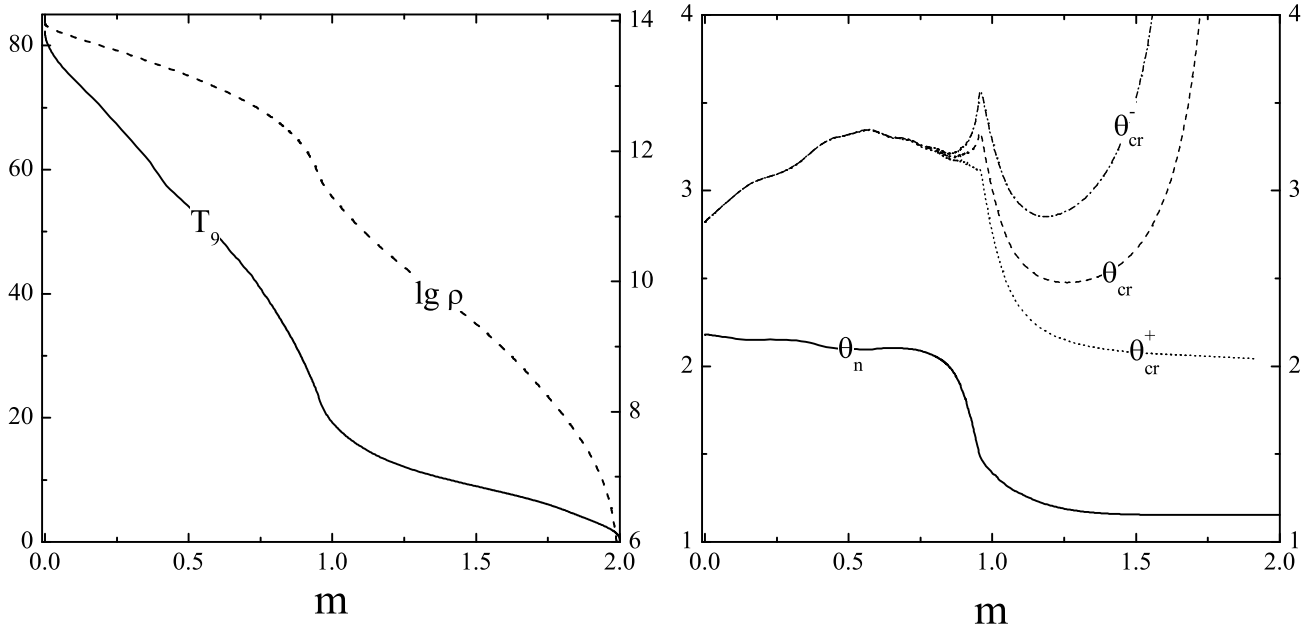

FIG. 3. (a: left) Temperature (solid curve, left axis) and logarithm of the density (dashed curve, right axis) versus mass coordinate $m = M/M_\odot$ inside the collapsing stellar core. (b: right) Degree of neutronization $\theta_{\rm n}$ and its critical values with allowance for the $\nu_{\rm e}-\nu_{\rm e}$ scattering.

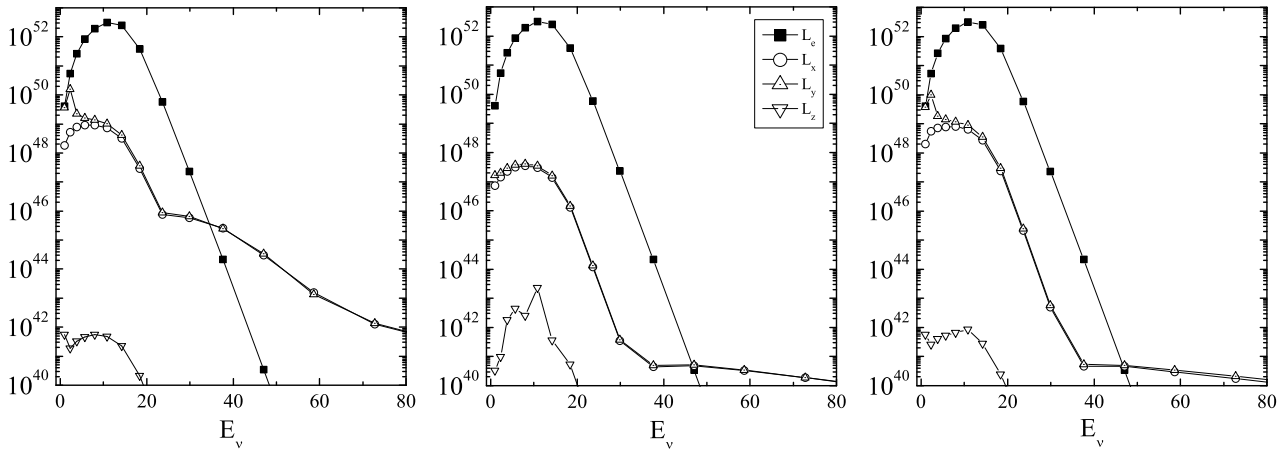

FIG. 4. Spectral luminosities L_ν (erg s^{-1} MeV^{-1}) of sterile neutrinos leaving the collapsing stellar core. The calculations (a: left) without $\nu_{\rm e}-\nu_{\rm e}$ scattering, (b: center) with isotropic scattering, and (c: right) with anisotropic scattering.

produced in the deepest and hottest regions of the stellar core. On the whole, the StN yield is smaller than the yield of the active component (electron neutrinos) by more than two orders of magnitude. At high energies ($E_\nu \gtrsim 40$ MeV) the spectral luminosity of the sterile component begins to dominate.

Let us now consider the scattering effect. Comparison of Figs. 4a and 4b shows that the absence of a resonance reduces considerably the StN yield. Indeed, $\theta_{\rm cr}$ when the $\nu_{\rm e}-\nu_{\rm e}$ scattering is taken into account is too large compared to the typical $\theta_{\rm cr} = 2$ (see Fig. 3b). Allowance for the anisotropy (Fig. 4c) gives a mixed spectrum: the range of low energies is analogous to the case without scattering; the high–energy spectrum (the so–called "pedestal") is suppressed, as in the isotropic case. This is explained by a combination of two effects: first, different generation depths of neutrinos

with different energies (high–energy StN are generated in deep layers of the core) and, second, the dependence of the resonant enhancement of oscillations on the neutrino energy. To demonstrate this, we provide Fig. 5, which shows the

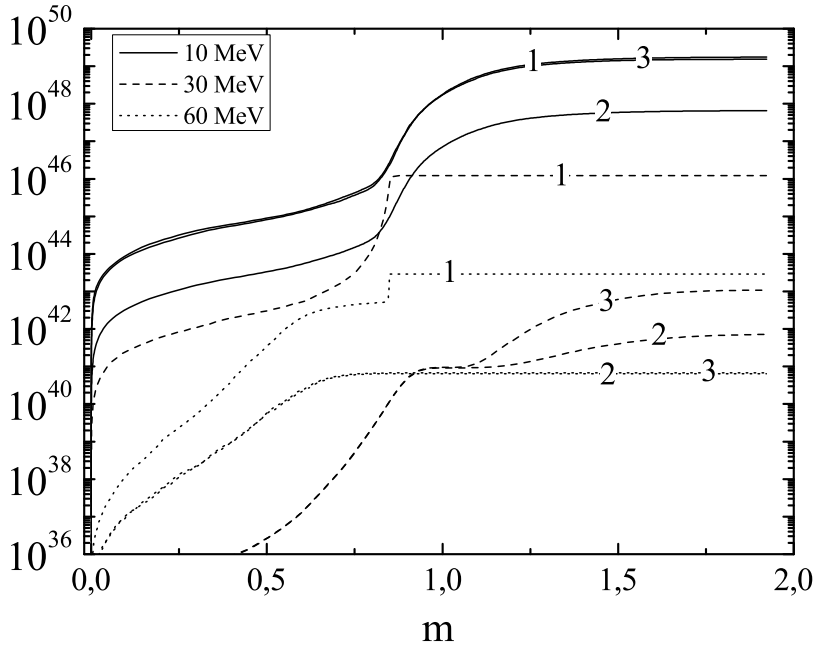

FIG. 5. Total local luminosities of sterile neutrinos $L_\nu(m)$ versus mass coordinate $m = M/M_\odot$ in the collapsing stellar core for $E_\nu = 10, 30$ and 60 MeV (the solid, dashed, and dotted curves, respectively). The numbers indicate the cases without scattering (1), with isotropic scattering (2), and with anisotropic scattering (3).

total spectral StN luminosities $L_\nu = L_\mathrm{x} + L_\mathrm{y} + L_\mathrm{z}$ as functions of the mass coordinate $m = M/M_\odot$ in the collapsing stellar core. The spectral luminosity at a given stellar radius r is defined via the local spectral flux by the formula $L_\nu = 4\pi r^2 F_\nu(r)$ (erg s^{-1} MeV^{-1}). The luminosities are shown for $E_\nu = 10, 30$ and 60 MeV (the solid, dashed, and dotted curves, respectively). The numbers mark the cases without scattering (1), with isotropic scattering (2), and with anisotropic scattering (3). The resonance region is easily seen on curves 1, but it is smeared at low energies. At an energy of 30 MeV (dashed lines) the resonance zone is still fairly wide and leads to an increase in the luminosity by almost two orders of magnitude (there is nothing of the kind on dashed curves 2 and 3, i.e., with scattering). At $E_\nu = 60$ MeV without scattering the resonance is narrow and leads to an increase in the luminosity approximately by a factor of 4, while the curves with scattering (2 and 3) exhibit a gradual rise without resonances.

Thus, the following conclusions can be reached: first, the $\nu_\mathrm{e}-\nu_\mathrm{e}$ scattering effect is very important in the calculations of the StN fluxes, because it changes the resonant degree of neutronization. In the case under consideration, the scattering has a negative effect on the generation of sterile neutrino components, but, as we will see below, this is not always the case. Second, the resonant enhancement of oscillations at the critical degree of neutronization pointed out in Khruschov et al. (2015) actually plays an important role under stellar core collapse conditions. Third, this effect depends strongly on the neutrino energy: for very high energies the resonance zone is too narrow (because the mean free path is small), while for low energies the effect itself is small. An optimum is probably reached in the energy range $E_\nu = (20 \div 40)$ MeV, which determines the region where a change in the pattern of the spectrum in Fig. 4, i.e., a transition to a more gradual drop in luminosity with energy (the "pedestal" effect), occurs.

THE POSTBOUNCE COLLAPSE PHASE

Let us now consider the supernova explosion phase that begins after an abrupt stop of the core collapse, bounce, and the generation of a diverging shock front that, having reached the outer stellar layers, must eject them, producing the observed explosion. The passage of the shock front through the matter heats it up, breaking all complex nuclei into free neutrons, protons, and α–particles. Abrupt neutronization of matter leading to $\theta_\mathrm{n} \sim 10$ also occurs in the postshock region. Consider this phase in detail.

In Fig. 6, which is analogous to Fig. 3, the parameters of the stellar core are shown at approximately 3 ms after

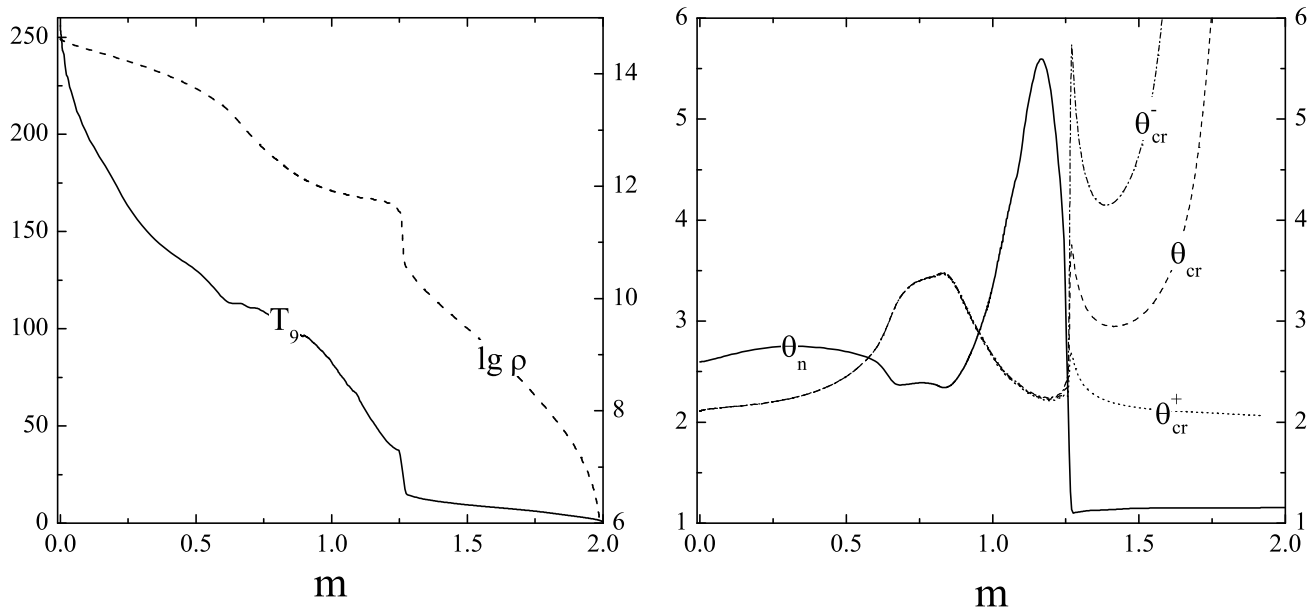

FIG. 6. Parameters in the core about 3 ms after bounce. (a: left) temperature (solid curve, left axis) and logarithm of the density (dashed curve, right axis) versus mass coordinate $m = M/M_\odot$ inside the collapsing stellar core. (b: right) degree of neutronization θ_n and its critical values with allowance made for the $\nu_\mathrm{e}-\nu_\mathrm{e}$ scattering.

bounce. The shock front seen from the jumps in all thermodynamic quantities is at $m \approx 1.25$. The matter in the region traversed by the shock front, i.e., in the range $0.8 \leq m \leq 1.25$, is strongly neutronized (see Fig.6b). The situation in the core after its bounce is seen to have changed significantly. Without $\nu_\mathrm{e}-\nu_\mathrm{e}$ scattering the curve $\theta_\mathrm{n}(m)$ still intersects the resonant value $\theta_\mathrm{cr} = 2$ only once at the shock front. However, with scattering $\theta_\mathrm{cr}(m)$ now intersects with the curve $\theta_\mathrm{n}(m)$ three times! The result can be seen in Fig. 7, which is analogous to Fig. 5 for the prebounce collapse phase, except that only two cases are presented here: without scattering and with anisotropic scattering. We will begin from $E_\nu = 10$ MeV (solid lines). The total spectral luminosities for cases 1 and 3 coincide up to the zone of the second resonance at $m \approx 0.95$, whereupon the luminosity with scattering increases by almost three orders of magnitude. The first resonance at $m \approx 0.57$ and the third one at the shock front do not give any noticeable enhancement of oscillations. At an energy of 30 MeV (dashed curves) for the case without scattering the resonance at $\theta = 2$ manifests itself at the shock. The first and the second resonances for case 3 are also clearly seen. They also work for an energy of 60 MeV (dotted curves), while for case 1 at this energy the resonance at the shock vanishes. All of this draws a complex picture of the resonant enhancement of oscillations whose properties depend on the stellar core parameters, the neutrino energy under consideration, and the included oscillation parameters.

The spectral characteristics of the fluxes of neutrinos leaving the stellar core at the instant of time under consideration are shown in Fig. 8. Just as in Fig. 4, the curve with filled squares indicates the spectrum of electron neutrinos. The small symbols and thin curves indicate the result of our calculation without $\nu_\mathrm{e}-\nu_\mathrm{e}$ scattering; the large symbols and thick curves represent our calculation with anisotropic scattering. In principle, the StN spectrum without $\nu_\mathrm{e}-\nu_\mathrm{e}$ scattering is very similar to the results of our calculation with the profile before bounce discussed above, while the spectrum with anisotropic scattering differs significantly. First, it exhibits some oscillations between the x and y StN components (their sum demonstrates a much smoother behavior). Second, the spectrum itself is considerably harder, and the "pedestal" effect is not such pronounced. This is apparently explained by the presence of several resonances lying at different depths in the stellar core. The deeper the resonance region lies, the more energetic StN can be produced there in significant quantity, with all the reservations concerning the dependence of the oscillation strength on the neutrino energy made above. Despite a considerable complication of the picture of oscillations, the situation qualitatively remains as before: the maximum of the spectrum occurs at low energies $E_\nu < 20$ MeV, with the total luminosity of sterile components being lower than the luminosity of electron neutrinos by several orders of magnitude. However, at high energies ($E_\nu \gtrsim 50$ MeV) the StN spectrum falls off much more gently, and the StN luminosity exceeds the luminosity of the active component.

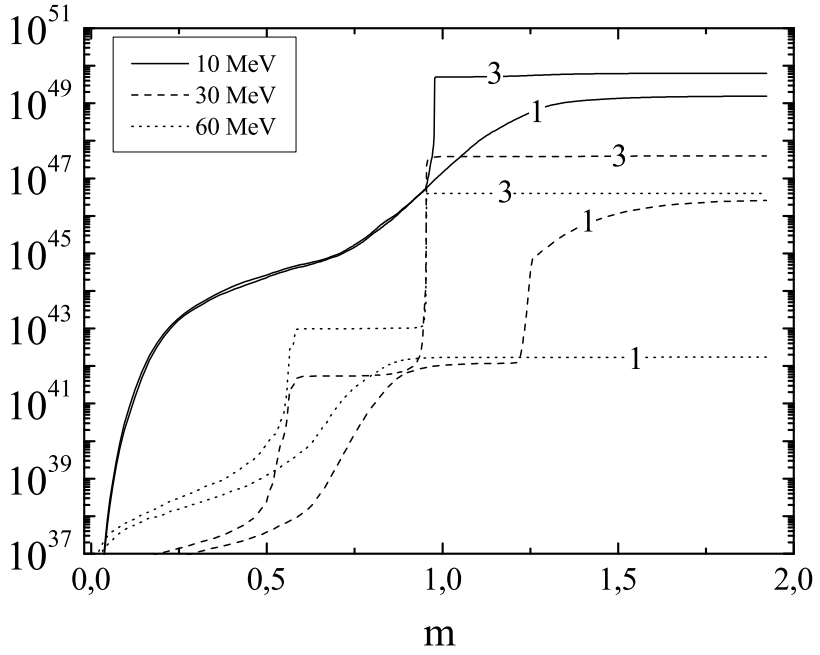

FIG. 7. Total local luminosities of sterile neutrinos $L_\nu(m)$ versus mass coordinate $m = M/M_\odot$ in the collapsing stellar core for $E_\nu = 10, 30$ and 60 MeV (the solid, dashed, and dotted curves, respectively). The numbers indicate the cases without scattering (1) and with anisotropic scattering (3).

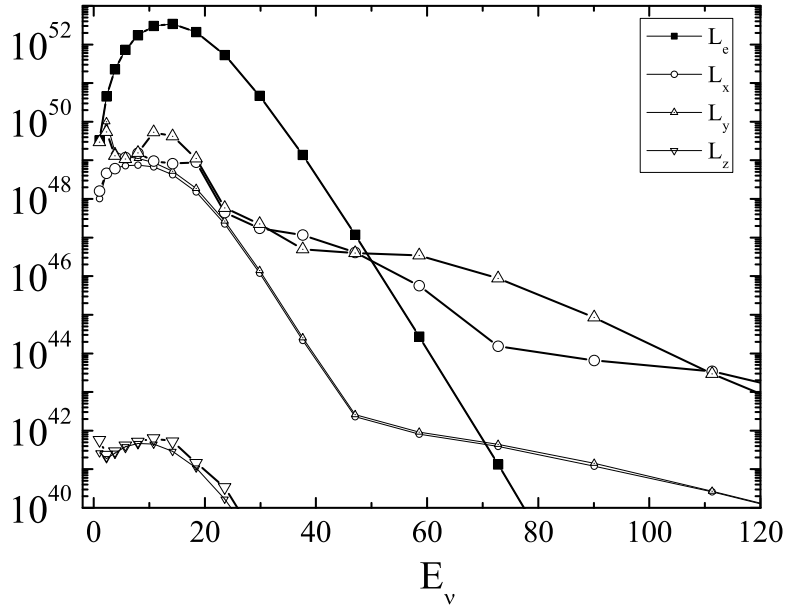

FIG. 8. Spectral luminosities L_ν (erg s^{-1} MeV^{-1}) of sterile neutrinos leaving the collapsing stellar core. The black filled squares indicate the spectrum of electron neutrinos. The small symbols and thin curves represent the calculation without ν_e–ν_e scattering; the large symbols and thick curves correspond to anisotropic scattering.

CALCULATIONS WITH OTHER PARAMETERS OF STERILE NEUTRINOS

The StN parameters that we used in our calculations as the "main" ones are not the only possible ones. It is very interesting to find out the possible influence of other sets of parameters (mixing angles, masses, etc.) on the properties of the resulting neutrino emission from supernovae. We will consider the case of inverted hierarchy (IH) of the neutrino mass spectrum as maximally differing from the "main" one. The question about the hierarchy of the active neutrino mass spectrum has not yet been solved; therefore, the IH case should be considered as an admissible one. We used the parameters for this case from Zysina et al. (2014) and Khruschov et al. (2015).

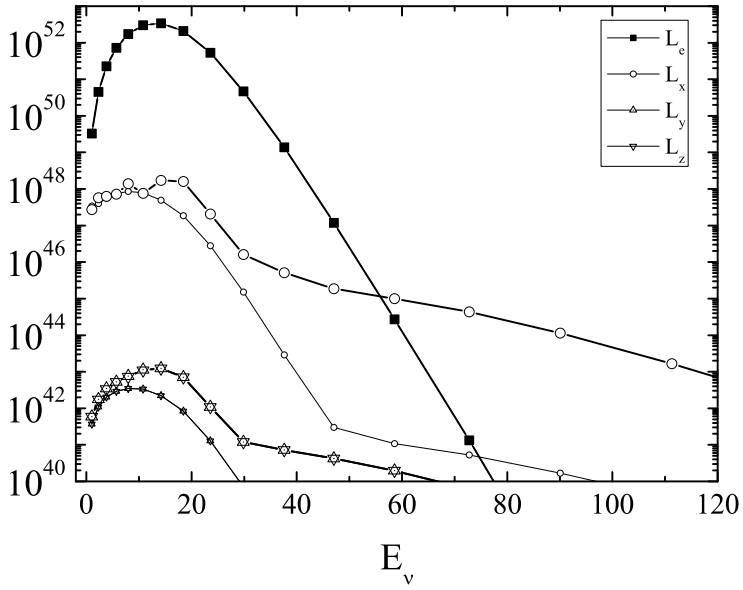

FIG. 9. Spectral luminosities L_ν (erg s^{-1} MeV^{-1}) of sterile neutrinos leaving the collapsing stellar core for the case of inverted hierarchy of the active neutrino masses. The black filled squares indicate the spectrum of electron neutrinos. The small symbols and thin lines represent the calculation without $\nu_e-\nu_e$ scattering; the large symbols and thick lines correspond to anisotropic scattering.

To demonstrate the influence of this set of parameters on the StN generation in a supernova, we will present the results of our calculations under the same supernova core conditions 3 ms after bounce as those in Fig. 6. Figure 9 shows the StN spectra for the IH case, with all designations being the same as those in Fig. 8. As can be seen, the picture is generally preserved. However, the yields of y– and z–type StN with almost the same value are now suppressed. This set of parameters leads to a reduction in StN generation by more than an order of magnitude, although the spectra are qualitatively very similar to the results of our calculations for the "main" NH case (see Fig. 8).

Apart from the consideration of other mixing parameters within the phenomenological oscillation model being investigated, a modification of the model itself is also possible, for example, by including the new hypothetical interaction between sterile neutrinos (see, e.g., Abazajian et al. 2012; Chu et al. 2015). This effect is capable of affecting the quantitative oscillation characteristics, but its study is beyond the scope of this paper.

CONCLUSIONS

In this paper we developed and implemented a combined algorithm for calculating the generation of sterile neutrinos inside the collapsing supernova core. It includes both a direct calculation of the neutrino oscillations and allowance for the generation, propagation, and interaction of neutrinos in a medium. This algorithm includes a separate consideration of both the region opaque to neutrinos (under neutrinosphere) and the semitransparent shell surrounding it. Basically, it is an efficient simplified method of calculating the oscillations in a medium that is applicable when the resulting yield of sterile neutrinos is small. Otherwise, the complete system of kinetic equations for all neutrino

flavors (see, e.g., Rudzsky 1990) should be solved.

Admittedly, the main result of our calculations is the demonstration that the derived energy characteristics of the StN flux are relatively small: for example the total StN luminosity turns out to be at least several orders of magnitude lower than the luminosity of electron neutrinos. In this way, we not only confirmed the applicability of the algorithm under consideration but also showed that sterile neutrinos, in contrast to the assumption made by Hidaka and Fuller (2006, 2007), are incapable of affecting significantly the collapse. At least, this is true for the parameters and the oscillation model we considered.

An important result of our calculations is the proof that the resonant enhancement of StN oscillations noted previously in Khruschov et al. (2015) actually occurs inside the collapsing star. Each such resonance is capable of increasing the luminosity by several orders of magnitude. We also showed that the $\nu_e - \nu_e$ scattering effect could affect significantly the radiation parameters of the sterile component. In particular, at the postbounce phase it leads to an increase in the number of resonances in degree of neutronization.

Besides, we showed that the choice of other StN model parameters (hierarchy, mixing angles, neutrino masses) could affect significantly the parameters of the StN flux. We are going to systematically study the domain of experimentally and theoretically admissible parameters that maximize the yield of the sterile component. This will allow us to give the final answer to the question of whether StN can affect the collapse dynamics and parameters. However, the peculiarities of the StN spectra themselves (namely their significant hardness at high energies) seem to be of interest from the viewpoint of detecting the neutrino signal from supernovae at ground-based facilities.

In conclusion, let us discuss the influence of the supernova model used. We considered the collapse of an iron stellar core with a mass of $2M_\odot$, the so-called "hot" collapse typical of very massive stars with a mass $M \gtrsim 25M_\odot$. Lower-mass stars ($M \sim 15M_\odot$) have an iron core with a mass of $1.4M_\odot$ experiencing "cold" collapse running with lower electron capture rates and, hence, with smaller neutronization of matter (see, e.g., Blinnikov and Okun 1988). As a result, at the prebounce phase θ_n will lie even farther from the resonant value, and, hence, the yield of sterile neutrinos for cold collapse will be suppressed. In contrast, at the postbounce phase, as we saw, sterile neutrinos are generated mainly in the regions of multiple intersections of the degree of neutronization θ_n with its resonant value. As a consequence, the yield of sterile neutrinos must have close values for both cold and hot collapse. The same is also true for the characteristics of the emitted active (electron) neutrinos within the first several tens of milliseconds after bounce (see Liebendörfer et al. (2004) where the characteristics of the active neutrino emission from collapsing $13M_\odot$ and $40M_\odot$ stars are compared). As regards the "thermal" postbounce phase (hundreds of milliseconds), since active neutrinos and antineutrinos of all flavors are emitted here in approximately equal numbers, investigating the generation of sterile neutrinos under these conditions requires a special consideration.

ACKNOWLEDGMENTS

This study was supported in part by the Russian Foundation for Basic Research (project №14-22-03040 ofi-m). A.V. Yudin and D.K. Nadyozhin also thank the Russian Science Foundation (grant №14-12-00203) for financial support in the part of this work concerning the calculation of the characteristics of active neutrinos. We are grateful to the referees for constructive remarks.

REFERENCES

[1] K.N. Abazajian, M.A. Acero, S.K. Agarwalla, A.A. Aguilar-Arevalo, C.H. Albright, S. Antusch, C.A. Argüelles, A.B. Balantekin, et al., arXiv:1204.5379[hep-ph] (2012).
[2] P.A.R. Ade et al. [Planck Collaboration], Astron. & Astrophys. **571**, A16 (2014).
[3] S. Antusch and O. Fischer, J. High Energy Phys. 2014(10), 094 (2014).
[4] S.I. Blinnikov, L.B. Okun, Sov. Astron. Lett. **14**, 368 (1988).
[5] A. Boyarsky, O. Ruchayskiy, D. Iakubovskyi, and J. Franse, Phys. Rev. Lett. **113**, 251301 (2014).
[6] E. Bulbul, M. Markevitch, A. Foster, R.K. Smith, M. Loewenstein, and S.W. Randall, Astrophys. J. **789**, 13 (2014).
[7] A. Burrows and T.A. Thompson, arXiv:astro-ph/0211404 (2002).
[8] L. Canetti, M. Drewes, and M. Shaposhnikov, Phys. Rev. Lett. **110**, 061801 (2013).
[9] F. Capozzi, G.L. Fogli, E. Lisi, A. Marrone, D. Montanino, and A. Palazzo, Phys. Rev. D **89**, 093018 (2014).
[10] X. Chu, B. Dasgupta, and J. Kopp, J. Cosmology Astropart. Phys., Issue 10, 011 (2015).
[11] J.M. Conrad, C.M. Ignarra, G. Karagiorgi, M.H. Shaevitz, and J. Spitz, Adv. High Energy Phys. **2013**, 163897 (2013).

[12] M. Drewes and B. Garbrecht, arXiv:1502.00477 [hep-ph] (2015).
[13] D.S. Gorbunov, Physics-Uspekhi **57**, 503 (2014).
[14] A. de Gouvêa, Phys. Rev. D **72**, 033005 (2005).
[15] C. Giunti, M. Laveder, Y.F. Li, and H.W. Long, Phys. Rev. D **88**, 073008 (2013).
[16] J. Hidaka and G. Fuller, Phys. Rev. D **74**, 125015 (2006); ibid. **76**, 083516 (2007).
[17] C.M. Ho and R.J. Scherrer, Phys. Rev. D **87**, 065016 (2013).
[18] S. Horiuchi, B. Bozek, K.N. Abazajian, M. Boylan-Kolchin, J.S. Bullock, S. Garrison-Kimmel, and J. Onorbe, arXiv:1512.04548 [astro-ph.CO].
[19] Q.-G. Huang, K. Wang, and S. Wang, arXiv:1512.05899 [astro-ph.CO] (2015).
[20] L.N. Ivanova, V.S. Imshennik, and D.K. Nadyozhin, Nauch. Inform. Astron. Sov. AN SSSR 13, 3 (1969).
[21] V.S. Imshennik, D.K. Nadezhin, Sov. Phys.–JETP **36**, 821 (1973).
[22] V.V. Khruschov, Phys. Atom. Nucl. **76**, 1356 (2013).
[23] V.V. Khruschov and S.V. Fomichev, arXiv:1310.5817v3 [hep-ph] (2015).
[24] V.V. Khruschov, S.V. Fomichev, O.A. Titov, Phys. Atom. Nucl. **79**, Issue 5, 708 (2016).
[25] V.V. Khruschov, A.V. Yudin, D.K. Nadyozhin, and S.V. Fomichev, Astron. Lett. **41**, 260 (2015).
[26] E. Komatsu et al. [WMAP Collabration], Astrophys. J. Suppl. Ser. **192**, 18 (2011).
[27] J. Kopp, P.A.N. Machado, M. Maltoni, and T. Schwetz, J. High Energy Phys. 2013(05), 050 (2013).
[28] M. Liebendörfer, Astrophys. J. **633**, 1042 (2005).
[29] M. Liebendörfer, O.E.B. Messer, A. Mezzacappa, S.W. Bruenn, Ch.Y. Cardall, and F.-K. Thielemann, Astrophys. J. Suppl. Ser. **150**, 263 (2004).
[30] D.K. Nadezhin, I.V. Otroshchenko, Sov. Astron. **24**, 47 (1980).
[31] K.A. Olive et al. [Particle Data Group], Chin. Phys. C **38**, 090001 (2014).
[32] S.T. Petkov, I. Girardi, and A.V. Titov, Int. J. Mod. Phys. A **30**, 1530035 (2015).
[33] M.A. Rudzsky, Astrophys. Space Sci. **165**, 65 (1990).
[34] T. Schwetz, M. Tórtola, and J.W.F. Valle, New J. Phys. **13**, 063004 (2011).
[35] I. Tamborra, G.G. Raffelt, L. Hüdepohl, and H.-T. Janka, J. Cosmology Astropart. Phys., Issue 1, 013 (2012).
[36] M.-K.L. Warren, M. Meixner, G.Mathews, J. Hidaka, and T. Kajino, Phys. Rev. D **90**, 103007 (2014).
[37] M.-R. Wu, T. Fischer, L. Huther, G. Martínez-Pinedo, and Y.-Z. Qian, Phys. Rev. D **89**, 061303(R) (2014).
[38] A. V. Yudin, Cand. Sci. (Phys. Math.) Dissertation Inst. Theor. Exp. Phys., Moscow, (2009).
[39] A.V. Yudin, D.K. Nadyozhin, Astron. Lett. **34**, 198 (2008).
[40] N.Yu. Zysina, S.V. Fomichev, V.V. Khruschov, Phys. Atom. Nucl. **77**, 890 (2014).